

PHYSICAL REVIEW B

CONDENSED MATTER

THIRD SERIES, VOLUME 38, NUMBER 1

1 JULY 1988

5*f*-band width and hybridization in uranium silicides

D. D. Sarma,* S. Krummacher, and F. U. Hillebrecht[†]

Institut für Festkörperforschung, Kernforschungsanlage, D-5170 Jülich, Federal Republic of Germany

D. D. Koelling

Materials Science Division, Argonne National Laboratory, 9700 South Cass Avenue, Argonne, Illinois 60439

(Received 7 August 1987; revised manuscript received 12 February 1988)

X-ray-photoemission spectroscopy and bremsstrahlung-isochromat spectroscopy are utilized to examine the series of uranium silicides U_3Si_2 , USi , USi_2 , and USi_3 . Maintaining the same ligand, this set of materials progresses from the case where direct *f*-*f* interaction is possible to one where only *f*-ligand interactions can occur. It is found that, while the results are dominated by the properties of the measurement techniques, there is evidence for *f*-band broadening with increasing ligand interactions.

INTRODUCTION

A central focus in electronic-structure studies for actinide materials, dating all the way back to debate on the actinide and thoride hypotheses, is the question of localization of the *f* states. The question was very early recast in terms of the competition between the intra-atomic repulsion of the *f* orbitals (U_{ff}) and the formation of band states "of width W ." (U_{ff}/W) then becomes the parameter controlling the physics, such that itinerant behavior is observed when it is small and local behavior when it is large. While really only valid for a system consisting of a single doubly degenerate orbital coupled to a single band, it does convey the proper behavior. U_{ff} is approximately fixed by the choice of actinide—in our case, uranium with $U_{ff} \sim 2\text{--}2.5$ eV. The bandwidth W is thus the more easily varied factor of this parameter. In this paper, it is the bandwidth part of the parameter that is to be studied by exploiting the rich phase diagram of the silicides.

There are a number of mechanisms by which *f* levels can be broadened into bands. Itinerant behavior is more prevalent in the actinides because the tail of the 5*f* orbital extends further out of the core region of the actinide than does that of the 4*f* orbital in a comparable rare-earth material.¹ Initial interest centered on the fact that, in many cases, actinide ions were actually sufficiently close together that the *f* orbitals could form a tight-binding band on their own.^{1–5} This led Hill to propose his now famous correlation of itinerant behavior (characterized through superconductivity or magnetism) to actinide separation.⁵ That correlation shows that for uranium materials with interactinide separations less than

about 3.4 Å, magnetic behavior does not occur except when iron or nickel is present to drive it. Most magnetic materials have a uranium separation greater than 3.6 Å. Such a correlation is easily understood because the small size of the *f* orbitals limits the range of their interactions. But perhaps the most useful aspect of the Hill plot is its exceptions—which highlight those materials which have large uranium separations and yet are not magnetic: Itinerant behavior is being induced into the *f* states of these materials by interactions with the remaining non-*f* conduction electrons. This is certainly not an idea unique to *f*-orbital materials as it is well known in the transition-element materials⁶ with nearly local *d* shells. It also occurs in the small-separation regime of the Hill plot among the Ce cubic Laves phases—but that is not as easy to spot.⁷ These hybridizing *f*-state materials are the more interesting ones because it is hybridization which persists into the transition to localized behavior that produces mixed-valent and heavy-fermion behavior. Besides the differing dependence on interatomic separation, other differences arise when the *f* orbitals interact with the other conduction electrons rather than themselves. As will be seen below, if the remaining conduction-electron orbitals have very small spin-orbit coupling (such as in Si), hybridization with those orbitals provides a mechanism to mix $f_{5/2}$ and $f_{7/2}$ so that the spin-orbit splitting is significantly reduced. While no *k* dependence is observed in these experiments, the direct *f*-*f* interaction will be more prevalent near the Brillouin-zone center and edges whereas hybridization with other orbitals will be more prevalent in the interior of the irreducible wedge.

Many examples of hybridizing *f*-state-like behavior occurring at large actinide separation are found in materials with the $L1_2$ structure. USi_3 is an excellent exam-

TABLE I. Selected crystallographic data for the compounds studied (from Ref. 9).

Compound	Structure	U-U sep.	Coordination	U-X sep.	Coordination
U ₃ Si ₂	U ₃ Si ₂	U(1) 3.32	8	2.97	2
		U(2) 3.32	4	2.90	2
				2.93	4
USi	FeB	~3.60	7	~2.95	7
USi ₂	AlB ₂	3.85	6	3.02	12
USi ₃	Cu ₃ Au	4.04	6	2.86	12
UIr ₃	Cu ₃ Au	4.02	6	2.84	12

ple of this. One controlled way to study hybridization effects is thus to compare various materials within this structure.⁸ In such an approach, one varies the “ligand” atom and observes the resulting change in properties. Interpretation is somewhat hampered by uncertainty as to just what salient feature or features have been varied since one is varying atomic size, electronegativity, polarizability, and atomic orbital makeup all at once. Alternatively, we examine here a different coordinate by keeping the “ligand” atom fixed and looking at different ordered compounds of the phase diagram: U₃Si₂, USi, USi₂, and USi₃. These silicides are characterized in Table I. In this case, the chemical properties of the ligand are held constant and it is nearest-neighbor distance, coordination number, and geometrical arrangement which are the varied factors. In U₃Si₂, the actinide separation is actually small enough for direct f - f interaction to occur. As the actinide (i.e., U) separation is increased, the direct f - f interaction will become much less significant. But the interaction of the f orbital with the p orbitals of the surrounding ligand (i.e., Si) atoms will continue. A very simple synopsis of these expectations is presented in Table II. There, it is assumed that the strength of an individual atomic interaction between orbitals of angular momentum l and l' separated by a distance R varies as $R^{-(l+l'+1)}$. By comparing the values for the product of the near-neighbor coordination number with this radial factor, one obtains a rough index for the variation in relative importance of the interactions. Much is neglected in this index so Table II should be taken only as a very rough guide. Examining Table II, one expects the strength of the direct f - f interaction to drop precipitous-

TABLE II. Relative strength of the f - f interactions and the f - p interactions on the basis of an extreme-tight-binding model applied to the data of Table I (see text).

Material	Direct f - f strength	f - p interaction strength
U ₃ Si ₂	1 ^a	1 ^a
USi	0.66	0.83
USi ₂	0.36	1.28
USi ₃	0.26	1.68

^aDefined as one to set the scale. U-U coordination number taken as the average for the two inequivalent sites.

ly as one increases the relative proportion of Si. U₃Si₂ is well within the itinerant f -state range on the Hill plot so that the f - f interaction must be strong enough to form bands by itself. USi already has a considerably reduced direct f interaction strength and falls at the large separation boundary of the transition region between itinerant and local behavior in the Hill plot. Any direct f - f interaction can have only a very minor effect in the remaining two materials. As for the f - p interaction, U₃Si₂ and USi should have very comparable strengths with USi₂ and USi₃ exhibiting stronger interactions. This is consistent with the $L1_2$ structured materials, including USi₃, having provided very fertile ground for the study of hybridization effects. Thus the series represents a rapidly diminishing f - f interaction with a growing f - p interaction. (This, of course, only reflects the ground state.) Finally, it should be mentioned that a U f - d interaction has not been considered because it occurs on-site only at very low symmetry and a second-nearest-neighbor interaction of this type is generally not favored.

The primary information to be sought is the variation in f -band width amongst the various silicides. To examine bandwidths, the tools of choice are x-ray-photoemission spectroscopy (XPS) to examine the occupied part of the bands and bremsstrahlung-isochromat spectroscopy (BIS) to examine the unoccupied portion. This is a well-established practice.¹⁰⁻¹⁹ This must be done with some caution, however, since the probe (photon or electron) is of quite high energy and may involve the properties of the excited states. There are three cases where these spectra represent the band density of state convoluted with matrix-element effects: (1) in the sudden approximation (often assumed in using electron spectroscopy for chemical analysis) where the remaining electrons are assumed not to have time to respond before the photoelectron is removed—this is rather unlikely;²⁰ (2) the itinerant or band case where the excitation is so spread out that the electronic distribution differs negligibly from the ground state—also unlikely for the f electrons here; and (3) the fully screened case where the locally excited state is immediately very well screened. This is most likely the case for the data to be presented here. In this well-screened case, an f orbital vacated by the excited electron is screened by the population of (possibly) other f orbitals. For this to occur, the material must have a sizable hopping matrix element so that, although the process is different, it is hard to distinguish this case from case (2), the extended or band excitation. However, in

this third case, there can be energy shifts associated with the differing energetics of the screening charge, but they should be small. (This well-screened case is roughly equivalent to the induced Fermi surface peak in the Anderson model.)

Finally, it is necessary to consider the possibility of satellite structure (the $f^n \rightarrow f^{n-1}$ or primary peak of the Anderson model) although the silicides have been chosen as being very unlikely candidates for such an occurrence. The primary interest in actinide materials is after all the f -orbital quasilocal behavior and one manifestation of locality, at least in the excitation spectrum, is indeed the presence of satellite structure. The two-peak structure appearing in both the XPS and BIS Ce compound f spectra is now quite famous with an extensive literature. In the actinides, satellite structure has been identified in BIS for UIr_3 .¹² Evidence for XPS satellite structure is much weaker although it is claimed that a very weak broad peak about 1 eV below the Fermi energy can be discerned by considering the systematic variation through many compounds.^{21,22} Certainly, it has been observed that the experimental widths are larger¹⁴ than calculated band-structure widths. In the case of the silicides, there is significant detail derived from uranium d -band structure (which we have tried to model in the Appendix) as well as possible Si Auger structure (only viewed as "other") appearing in this important 1 eV region. The consequence is that little can be said about the presence of satellite structure or broadening, but its possible presence coupled with these other two phenomena precludes a determination of the f -band width by straightforward observation of its lower bound.

For the XPS photon energies used (1486.6 eV), matrix-element effects, shown for the isolated-atom case in Table III, strongly select the f character—which is the object of interest. This fact has long been the basis for using high energy XPS to look for f character. Consequently, one expects to see primarily the f density of states but skewed by a mild energy dependence of the matrix elements, broadened by electron-electron scattering and instrumental resolution, modulated by the thermal Fermi factor, and blurred by secondary emission. The Auger-like electron-electron scattering induces a broadening that increases as the square of the separation of the level from the Fermi energy²⁴ and can cause the measured spectrum to appear considerably broader than the band density of states (a fact apparently not fully appreciated in Ref. 14). These must also be considered in

interpreting the results in light of the fact that the experimental resolution seriously obscures the information sought. This has been modeled in the Appendix. The BIS also has f selectivity and a similar collection of impeding phenomena. These have been (less well) considered in the Appendix.

In the next section, the raw experimental results are reported. A more speculative discussion of the data appears in the following section. There it is argued that although the information sought is very nearly washed out, one obtains some evidence through a careful examination of the relative behavior of the two spin-orbit split peaks. It is amusing to note that the interpretation argues a reversal in behavior from what one would initially conclude.

EXPERIMENTAL RESULTS

The polycrystalline samples and were produced by inductive melting of the appropriate quantity of the constituents in a levitation crucible under an argon atmosphere. Phase purity was verified by x-ray diffraction and U:Si ratio by XPS. The measured samples were cleaned *in situ* by scraping with a ceramic file in a vacuum maintained at pressures lower than 2×10^{-10} Torr. The XPS and BIS measurements were performed in a combined spectrometer¹⁰ having a resolution of 0.6 eV full width at half-maximum (FWHM) for XPS. The BIS resolution function is more complex. Using a standard Fermi edge assessment, it was found to consist of an 0.75 eV Gaussian plus an 0.2 eV Lorentzian. The silicide XPS spectra are presented collectively in Fig. 1 and the BIS spectra in Fig. 2.

Comparing the XPS spectra for the various silicides, one finds that the curves are very nearly identical from the Fermi energy down to about -4 eV. There is a single sharp peak near the Fermi energy. This peak is almost precisely the same width in U_3Si_2 , USi , and USi_2 . In USi_3 , it is slightly broader. Each spectrum has barely discernible structure in the -2 to -4 eV range where there is definitely intensity beyond that expected as a tail from the peak. This extra structure is roughly comparable in each compound suggesting that it arises from the U d states since Si derived structure should vary with the Si to U ratio. For USi_3 , a very broad peak appears in the -5 to -12 eV range arising from the Si s bands. It can be reasonably simulated by a combination of a linewidth broadened s density of states and secondary emission correction and is also consistent with the observations¹⁷ in $\text{U}(\text{In}_x\text{Sn}_{1-x})_3$. This feature is not distinguishable in the other three materials most likely because of the reduced proportion of Si.

Following tradition, the Fermi energy in Fig. 1 has simply been placed at the half-intensity point. But that prescription for the placement of the Fermi energy is only strictly correct for a flat density of states cut off by a Fermi function and broadened. In these materials, the density of states in these compounds is far from flat at the Fermi energy which actually lies in the leading edge of a high peak derived from uranium f states. Consequently, the actual Fermi energy should be ~ 0.1 eV lower.

TABLE III. Ratio of atomic cross sections to that of the uranium f states at 1486.6 eV (from Ref. 23). Note that the effect will be somewhat less pronounced in the solid as discussed in the Appendix.

Orbital	Cross-section ratio
Si s	0.12
Si p	0.020
U d	0.017

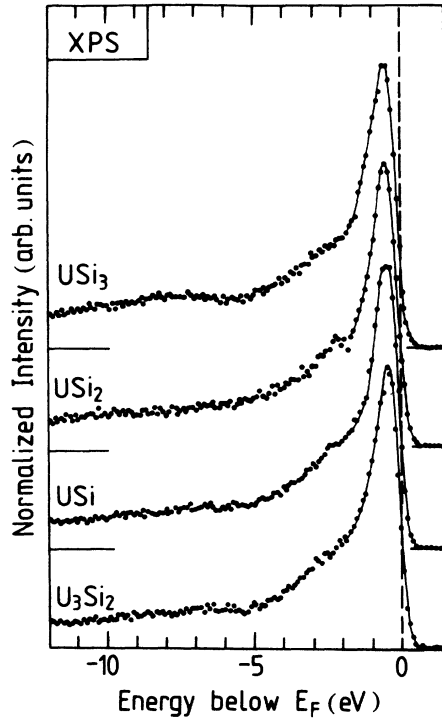


FIG. 1. XPS intensities for the four uranium silicides as marked.

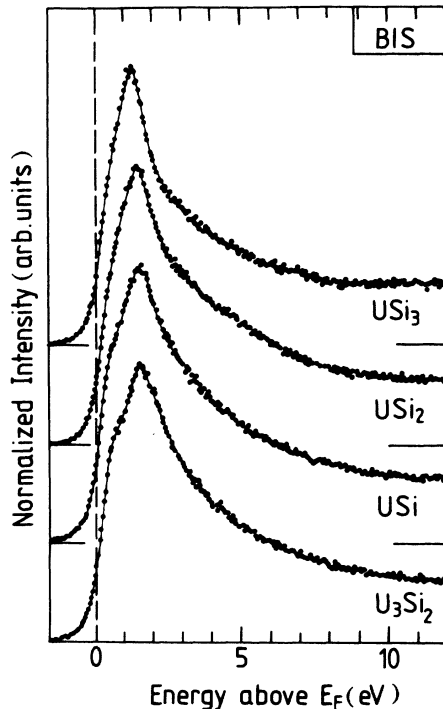


FIG. 2. BIS intensities for the four uranium silicides as marked.

The BIS spectra in Fig. 2 all exhibit a single peak roughly 1.5 eV above the Fermi energy with a tail extending to the higher energies. This peak position is slightly lower in USi_3 than for the other three materials. There is only a very slight variation amongst these three. In all four materials, but especially in U_3Si_2 and USi , a kink is evident on the low-energy side of this main peak. It would be tempting to identify this with a broadened Fermi level cutoff. While this was our own initial prejudice, it does not hold up under detailed simulation. It more likely arises from an $f_{5/2}$ - $f_{7/2}$ peak splitting. The tail reaching below the Fermi energy is quite broad and extends well beyond that to be expected from the quoted instrumental Gaussian broadening. This is the consequence additional Lorentzian factor mentioned above. The U_3Si_2 and USi spectra are essentially identical. There is a very slight narrowing evident in USi_2 while USi_3 is dramatically narrowed. The data shows no evidence for satellite structure as previously described¹² in the specific case of USi_3 .

DISCUSSION

Taking a conservative view of the XPS data, one would have to conclude that, at this experimental resolution, one cannot distinguish any change in bandwidth amongst U_3Si_2 , USi , and USi_2 and only a very small tentative increase in bandwidth for USi_3 if one uses the width of the major peak as one's index. As discussed above, one would certainly expect greater variation than this.

A possibly quite disturbing aspect is suggested by the attempted simulation of the spectrum for USi_3 where the partial density of states (PDOS) is available from band structure calculations. These are described in the Appendix. In USi_3 , the f -derived peak in the theoretically simulated spectrum actually appears at lower energy than the experimental peak which is very much contrary to expectations based on screening arguments. Based on the following considerations, this observation supports an assertion that strongly hybridized f orbitals are not as effective in emission as weakly hybridized f orbitals. The principal peak in USi_3 is actually derived from two peaks in the f PDOS: one arising from strongly hybridized f character roughly 1 eV below the Fermi energy, and one from the more weakly hybridized f character in a very large peak being cut off by the Fermi energy. In the simulation, broadening merges this lower peak with the upper one but with a maximum shifted to lower energy. That this is not observed in the experimental spectrum is most easily explained by a reduced weighting of the strongly hybridized contribution as was most dramatically seen²⁵ for UIr_3 . Certainly, matrix-element effects would act in this direction since the strongly hybridized f orbitals will have density shifted to larger radii away from the region of stronger dV/dr . However, that alone is unlikely to provide the large difference that appears to be needed here. Nonetheless, while certainly not proven or even understood, such an assertion would help provide an explanation as to why the XPS results should be so similar in these silicides as well as the negative results

found¹⁷ in the $U(In_xSn_{1-x})_3$ alloy studies.

The additional structure in the -2 to -4 eV range of the XPS is a consequence of the U d Si p hybridization. The possibility of U f satellite structure or Si Auger structure will be discounted here—although it must be admitted that this is somewhat cavalier. Wherever U hybridizes with p bands, the U d 's invariably hybridize into the bottom of the occupied band while the f 's hybridize in above at the Fermi energy. Again, USi_3 is perceptibly broader than USi_2 which is, in turn, just barely broader than the remaining two. This is consistent with the fact that USi_3 and USi_2 are the higher coordination number materials.

While the description given in this previous section of the BIS results is the strictly correct one, in this discussion a closer viewing very near the noise level will be utilized. Looking very closely at the spectra in Fig. 2, one still finds that USi is identical to U_3Si_2 but notes that USi_2 appears narrowed (in that the lower energy kink has been reduced and the initial falloff on the high energy side is faster) and that USi_3 is still narrower (and the only material with a significantly shifted peak). A possible interpretation of these observations is that the bands are narrowing in the manner of the decreasing f - f interaction. This, however, would be inconsistent with the interpretation of the XPS data where the USi_3 was suggested to have the marginally broader f bands. A simple downward motion of the f bands would entail a tremendous increase in intra-atomic Coulomb (Hubbard U) interactions through increased f count and thus should be discounted.

A possible resolution presents itself if one first focuses on the kinklike structure at the Fermi energy. The explanation of this structure is the Fermi energy truncation of the weaker $f_{5/2}$ peak which falls below the $f_{7/2}$ peak which is the dominant maximum. A more or less canonical result for the band structure of a material containing itinerant f electrons is the presence of these two broadened spin-orbit split peaks above the Fermi energy with a tail extending below the Fermi energy. It is this tail that accounts for the occupied itinerant f character. The states in the main body of the peaks are associated with very flat bands—i.e., more local, less hybridized states. In a very weakly hybridized system, the f peaks will be more clearly separated and the occupied f character will be very $f_{5/2}$ -like. However, as the hybridization with a light ligand such as Si is increased, $f_{7/2}$ character will be admixed into the $f_{5/2}$ peak until the situation approaches more nearly the case of a definite spin f state. (This is the situation for $CeSn_3$, for example.) In essence, one is blurring the $f_{7/2}$ character primarily downward due to the j mixing by the ligand. If this is the case, then the downward motion of the BIS peak is a measure of increased hybridization in USi_3 consistent with its being a Ll_2 structured material—a structure which exhibits more large separation-itinerant f -state cases than any other. This interpretation has been previously presented complete with a comparison to band calculations¹² except that there the example chosen for the more pronounced structures was UIr_3 . Please note that this argument does

not imply that the bandwidth of the other materials is narrower—only that the j mixing by hybridization is smaller. Direct f - f interactions would be more likely to preserve the j character. As the lower peak is pinned just above the Fermi energy, the upper peak position will be fixed by the spin-orbit splitting—which is approximately an atomic property. Any bandwidth effects then would have to be seen in the shape of the tails which is probably beyond resolution and clouded by other effects.

Here we must raise the same concern that was suggested for the XPS results. In modeling the BIS, there is structure that should be much more visible than it is (see Ref. 12). That structure arises from f character which is more strongly admixed with ligand states. Thus, one must consider the possibility that the states being sought will have a strongly reduced transition probability.

ACKNOWLEDGMENTS

We thank M. Campagna for his support of this work. One of us (D.D.K.) thanks A. J. Arko for helpful discussions. The work of one of us (D.D.K.) was supported by the U.S. Department of Energy, Office of Basic Energy Sciences, Division of Materials Science, under Contract No. W-31-109-ENG-38.

APPENDIX: MODELING OF THE SPECTRA

Here we briefly discuss some of the modeling that has been performed to try to gauge the significance of various features of the spectra. The intent was to assume the relevance of the partial density of states (which is available for USi_3) and determine how various effects would modulate it. It is to be pointed out that one effect not included was satellite structure which was assumed to be negligible. Thus, the effects being considered are all rather mundane and well known. The significance of the exercise is, in fact, to attempt to insure that the mundane not be mistaken for the exotic. The effects considered are now described in turn.

(a) The instrumental resolution was 0.6 eV FWHM for the XPS and 0.8 eV FWHM for the BIS (the additional Lorentzian was not included). This is represented by convoluting the theoretical spectrum with a Gaussian of that width. The instrument width actually determines the falloff at the Fermi energy rather than the thermal smearing. So, although the finite-temperature effects were incorporated, they will be ignored in this discussion. It is quite informative to do numerical experiments on this effect to see what could be learned by improvements in experimental resolution. What is suggested is that by halving the instrumental broadening one could discern that the central peak in USi_3 is split: the upper part being the cut off leading edge of a larger peak and the lower part a compound structure constructed from a peak about 0.5 eV below the Fermi energy with a shoulder arising from structure almost 1 eV below E_F . Further, the structure around -2 eV becomes much more clearly defined. (This observation is made in the presence of the level broadening discussed next but is dependent on the size of that effect—which is assigned empirically.)

(b) Electron-electron or lifetime level broadening was incorporated by convoluting the theoretical spectrum with a Lorentzian before applying the instrumental broadening. This presented some complication since the width chosen should represent the scattering rate from the band states. The dominant feature determining that rate is the available phase space for a particular energy. The approximation used was that this phase space, and therefore the scattering rate, increases as the square of the separation of the energy from the Fermi energy.²⁴ Consequently, the effect of structure in the density of states on this effect is omitted. Thus the level width Γ is given by

$$\Gamma = \alpha(e - E_F)^2,$$

where $\alpha \sim 0.1 \text{ eV}^{-1}$ must be assigned empirically. This has the correct property of going to zero at the Fermi energy and rising dramatically for energies away from it. Because the level broadening vanishes at the Fermi energy, the effect at the Fermi energy must be ascribed to the instrument broadening at these resolutions and temperatures.

(c) Secondary emission was accounted for by a simple prescription which is most easily applied to the experimental spectrum. The prescription (suggested by A. J. Arko) is to merely take the secondary emission at any energy as being proportional to the integral of all intensity—both primary and secondary—between that energy and the Fermi energy. This prescription assumes multiple scattering and differs from the more common practice of assuming a single scattering. The more standard single-scattering model is more easily applied to the theoretical model since its input should be the density of states. When applied to the experimental data, however, it requires an iterative solution. This multiple-scattering model, on the other hand, requires only a single step when applied to the experimental data. The truth, of course, lies somewhere between these two idealizations but, in light of the uncertainties involved, we opted for the more convenient model. The unknown proportionality constant in the model can be roughly determined for the XPS from the assumption that, at the lowest energy, all emission is due to secondaries. Doing so, one arrives at a proportionality constant of $0.032\text{--}0.036 \text{ eV}^{-1}$ for these samples. This correction sharpens up the Si s peak in USi_3 between -12 eV and -5 eV but otherwise changes little.

(d) Matrix-element effects are inserted in a strictly empirical manner with consideration given to calculated examples on the one hand and experimental observations on the other. Given that these adjustments are made to the best of one's ability, it is then important to see what discrepancies remain and try to understand why. Consider the atomic data quoted in Table II. That table indicates a dramatic reduction of the Si s - p and U d emission relative that of the U f which serves as a useful guide even though we know that the reduction is too severe for the solid. The logic is as follows: The matrix element (of $\epsilon \cdot p$) can easily be related to dV/dr by commuting with the Hamiltonian in the nonrelativistic approximation.²⁶ dV/dr peaks strongly in the deep core of the atom.

Whereas, in an atom, the orbitals can have long tails, the renormalized atom approach²⁷ tells us that the density in these long tails gets cut off in the solid with the attendant renormalization of the core region. This increases the matrix elements involving the more extended orbitals relative to those of the more compact orbitals over what is found in the atomic case. The effect will be rather more important for the uranium $6d$ states than for the Si $3p$ states. This would offer a possible explanation of the constancy of the -2 to -5 eV tail between the materials. At this resolution, the shape of the PDOS will do little to help in the analysis since the curves for the Si p and U d are very nearly indistinguishable in this -2 to -4 eV window. Another important observation is that one should expect a gradual decrease in the matrix element as the energy is lowered since, at least within the same band, the lower energy radial solutions have greater density in the outer region of the ion. The fact that the matrix elements should decrease is significant as the discrepancies appearing in Fig. 3 all are due to extra intensity at the lower energies.

The principal peak shows several very significant differences. To correct for the inappropriate assignment of the Fermi energy discussed above, the Fermi energy edge has been lined up by shifting the experimental curve upward 0.1 eV . This having been done, the match of the edge now merely reflects that our simulation of the instrument broadening is roughly correct. But this allows us to see that the peak of the theoretical curve is shifted to lower energy *relative to the edge* and does not reflect the shoulder barely evident in the experimental curve. One would normally expect the experimental peak to fall lower because of incomplete screening effects. In this case, however, the peak is actually derived from two

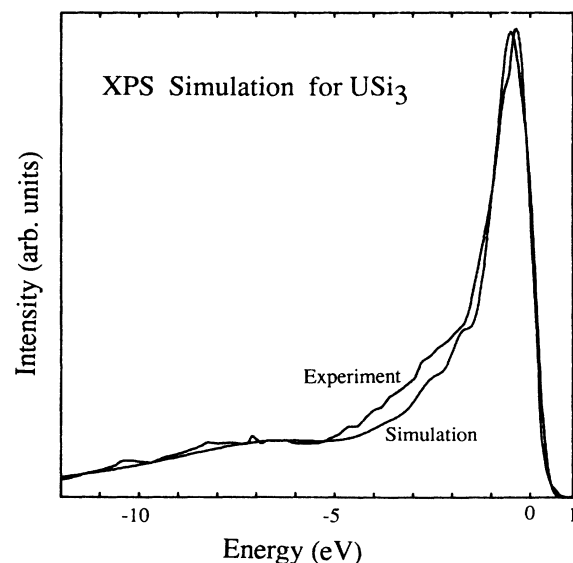


FIG. 3. Comparison to the experimental results of the best XPS simulation achieved for USi_3 following the prescription described in the Appendix.

peaks in the PDOS: one arising from strongly hybridized f character roughly 1 eV below the Fermi energy and more weakly hybridized f character in a very large peak which is being cut off by the Fermi energy. The comparison can be improved dramatically by making the ansatz that emission from the strongly hybridized f character is much weaker than it is from the weakly hybridized f

character. This would be very consistent with what is observed²⁵ in $U\text{Ir}_3$. Certainly matrix-element effects would act in this direction since the strongly hybridized f orbitals will have density shifted to larger radii away from the region of stronger dV/dr . However, they are alone unlikely to provide the large difference that appears needed here.

*Present and permanent address: Solid State and Structural Chemistry Unit, Indian Institute of Science, Bangalore 560012, India.

†Present address: Max-Planck-Institut für Festkörperforschung, D-7000 Stuttgart 80, Federal Republic of Germany.

¹A. J. Freeman and D. D. Koelling, in *The Actinides: Electronic Structure and Related Properties*, edited by A. J. Freeman and J. B. Darby, Jr. (Academic, New York, 1974), Vol. 1.

²E. A. Kmetko and J. T. Waber, in *Plutonium 1965*, edited by E. A. Kay and M. B. Waldron (Chapman and Hall, London, 1967).

³E. C. Ridley, Proc. R. Soc. London, Ser. A **247**, 199 (1958).

⁴H. L. Skriver, O. K. Andersen, and B. Johansson, Phys. Rev. Lett. **41**, 42 (1978); Phys. Rev. Lett. **44**, 1230 (1930).

⁵H. H. Hill, in *Plutonium and Other Actinides 1970*, edited by W. N. Miner (The Metallurgical Society of the American Institute of Mining, Metallurgical and Petroleum Engineers, New York, 1970).

⁶J. C. Fuggle, F. U. Hillebrecht, R. Zeller, Z. Zolnierrek, P. Bennett, and Ch. Freiberg, Phys. Rev. B **27**, 2145 (1983).

⁷D. D. Koelling, Physica **130B**, 135 (1985).

⁸D. D. Koelling, B. D. Dunlap, and G. W. Crabtree, Phys. Rev. B **31**, 4966 (1985).

⁹W. H. Zachariasen, Acta Crystallogr. **2**, 94 (1949).

¹⁰F. U. Hillebrecht, J. Keppels, and R. Otto, Rev. Sci. Instrum. **58**, 776 (1987); F. U. Hillebrecht, D. D. Sarma, and N. Martensson, Phys. Rev. B **33**, 4376 (1986).

¹¹D. D. Sarma, S. Krummacker, A. Wallash, and J. Crow, Phys. Rev. B **34**, 3737 (1986); F. U. Hillebrecht, D. D. Sarma, and N. Martensson, J. Magn. and Magn. Mater. **52**, 129 (1985).

¹²D. D. Sarma, F. U. Hillebrecht, W. Speier, N. Martensson, and D. D. Koelling, Phys. Rev. Lett. **57**, 2215 (1986).

¹³G. Landgren, Y. Jugnet, J. F. Morar, A. J. Arko, Z. Fisk, J. L.

Smith, H. R. Ott, and B. Reihl, Phys. Rev. B **29**, 493 (1984).

¹⁴J. W. Allen, S. J. Oh, L. E. Cox, W. P. Ellis, M. Wire, Z. Fisk, J. L. Smith, B. P. Pate, I. Landau, and A. J. Arko, Phys. Rev. Lett. **54**, 2635 (1985).

¹⁵R. D. Parks, M. L. denBoer, S. Raaen, J. L. Smith, and G. P. Williams, Phys. Rev. B **30**, 1580 (1984).

¹⁶J. Ghijsen, R. L. Johnson, J. C. Spirlet, and J. J. M. Franse, J. Electron Spectrosc. Relat. Phenom. (to be published).

¹⁷D. Sarma, S. Krummacker, W. Gudat, C. L. Lin, L. W. Zhou, J. E. Crow, and D. D. Koelling (unpublished).

¹⁸Y. Baer and J. K. Lang, Phys. Rev. B **21**, 2060 (1980).

¹⁹B. W. Veal and D. J. Lam, Phys. Rev. B **10**, 4902 (1974).

²⁰B. W. Veal and A. P. Paulikus, Phys. Rev. Lett. **51**, 1995 (1983); Phys. Rev. B **31**, 5399 (1985).

²¹A. J. Arko, B. W. Yates, B. D. Dunlap, D. D. Koelling, A. W. Mitchell, D. J. Lam, and Z. Zolnierrek, J. Less-Common Met. **133**, 87 (1987).

²²It has also been argued that an Auger channel could be responsible [see D. D. Sarma, F. U. Hillebrecht, C. Carbone, and A. Zangwill, Phys. Rev. B **36**, 2916 (1987)], but this assertion is also being questioned [see A. J. Arko, D. D. Koelling, C. Capasso, M. del Giudice, and C. G. Olson (unpublished)].

²³J. J. Yeh and I. Lindau, At. Data Nucl. Data Tables **32**, 1 (1985).

²⁴N. W. Ashcroft and N. D. Mermin, *Solid State Physics* (Holt, Rinehart, and Winston, New York, 1976), p. 347.

²⁵A. J. Arko, D. D. Koelling, and B. Reihl, Phys. Rev. B **27**, 3955 (1983).

²⁶J. F. Janak, A. R. Williams, and V. L. Moruzzi, Phys. Rev. B **11**, 1522 (1975).

²⁷L. Hodges, R. E. Watson, and H. Ehrenreich, Phys. Rev. B **5**, 3953 (1972).